JOURNAL OF THEORETICAL AND APPLIED MECHANICS
51, 1, pp. 131-141, Warsaw 2013

ON THE FIRST BOUNDARY VALUE PROBLEM OF THE PHOTOELASTIC THIN RING

Djelloul Rezini, Tawfik Tamine
University of UST-MB Oran, Faculty of Mechanical Engineering, Laboratoire LCGE, Algeria
e-mail: redjellou@yahoo.fr

Analytical solutions to the plane problems in terms of stresses for thin annular domains under compression loading are well known in several papers. Moreover, the large majority of the two-dimensional problems in the theory of elasticity are reducible to the solution of their boundary value problems. The two-dimensional photoelasticity methods easily provide the stress tensor components on the boundary, from one photograph only. The Beltrami-Michell equations with the Dirichlet photoelastic data state a well-posed hybrid problem in stress terms. It has been shown that the results obtained from the hybrid method developed in this paper, are applicable to any irregular shaped photoelastic domain of interest. Successful results have been obtained for more complicated forms and loads. The correctness of the results for the circular ring is confirmed and will be discussed in details.

Key words: photoelasticity, Beltrami-Michell equation, annulus

1. Introduction

The analysis of an annular thin disk subjected to diametral compression is often regarded as a problem of reference for verification and validation of theoretical or experimental techniques for stress or strain investigation of a study case, as done in (Navneet Kumar and Khobragade (2011) and Sciammarella and Gilbert (1973). Analytical solutions to the plane problems in terms of stresses for such annular domains under compression loading are well known in several papers (Nomura *et al.*, 2008; Filon, 1924). However, the concern of this paper is to show another way that exists in addition to those reference works listed by Tokovyy *et al.* (2010) for evaluating the stress state acting in a thin ring subject to diametral compression. Although the method developed in this study is not limited exclusively to this shape of structure, successful results have been obtained for more complicated forms and loads.

Moreover, the large majority of the two-dimensional problems in the theory of elasticity are reducible to the solution of their boundary value problems. We shall be concerned only with those solutions in which the components of the stress tensor are continuous and single-valued throughout the region $\Omega \cup \Gamma$ (Ω is the volume and Γ is the envelope surface) together with their first and second partial derivatives with respect to field variables. Moreover, the harmonic state of the stress invariant satisfies the Laplace equation, and is usually used to determine the interior potential of the stress sum if boundary values are known. It is well-known that each stress component is governed by the Beltrami-Michell equation (Timoshenko and Goodier, 1970). In fact, the source function of each Beltrami-Michell equation is expressed in terms of partial derivatives of the second order of the stress sum harmonic function. Therefore, the plane stress resolution is reduced to solving two Dirichlet problems successively.

In spite of some apparent disadvantages, photoelasticity often serves as a useful complement to numerical analyses, especially for validation of complex stressed models or when the boundary conditions are difficult to model. The two-dimensional photoelasticity methods easily provide the

stress tensor components on the boundary, from one photo only (see Kuske, 1979). The Beltrami-Michell equations with the Dirichlet photoelastic data state a well-posed hybrid problem in terms of stress, as done by Rezini (1984). The purpose of the present study is summarized as follows: the Beltrami-Michell equations are discretized in terms of finite difference equations to provide harmonic solutions of each stress component in any irregular shaped photoelastic domain.

To realize this objective, the present paper is organized in sections. In Section 2, the statement of the problem and the expressions of stresses in two dimensions are reviewed in a convenient form for the analysis purpose. The photoelasticity proceeding and its associated boundary values will be briefly described in Section 3. The numerical resolving of the photoelastic boundary value problem in any domain geometries is presented in Section 4. Before conclusion, the results will be discussed in details in Section 5.

2. Statement of the stress problem

The difficulty in analysis of stresses and strains in structural engineering depends on the complexity of the form and load of the structure parts and of the given specific conditions. Furthermore, from the strength of material point of view, the state of stresses is more useful for engineers. The equilibrium equation, the compatibility condition, and the material law are the three fundamental concepts of the theory of structures (Boresi *et al.*, 2011). However, the theory of elasticity proposes two strategies to minimize the analysis. The first one provides analytical solutions to plane strain and plane stress problems and can be obtained by using several techniques which use functions to reduce the unknown of governing equations. The stresses are written in terms of this new function (Ugural and Fenster, 2011).

According to the plane stress assumption in the absence of body forces, this problem is governed by the necessary and sufficient equilibrium conditions (Hetnarski and Ignaczak, 2011). The planar version of the equilibrium conditions are conveniently written with Greek indices as follows

$$\sigma_{\alpha\beta,\beta} = 0 \tag{2.1}$$

The stress function formulation is based on the idea representing the stress fields that satisfy the equilibrium equations. It is clear that equations (2.1) represent the necessary and sufficient condition for the existence of the function ψ, such that in absence of body forces the components of stresses are its partial derivates of thesecond order

$$\sigma_{\alpha\beta} = -\frac{\partial^2\psi}{\partial x_\alpha \partial x_\beta} + \delta_{\alpha\beta}\frac{\partial^2\psi}{\partial x_\kappa \partial x_\kappa} \tag{2.2}$$

where $\alpha, \beta, \kappa = 1, 2$ and the Kronecker delta δ_{ij} define the components of the identity matrix. Note that the summation over the repeated Greek indices should be done. The Airy stress function ensures that the stresses according to (2.2) satisfy equilibrium conditions (2.1). This is a necessary condition but not sufficient. The function ψ should also ensure that the compatibility and boundary conditions are satisfied. The introduced harmonic stress function obeys the Laplace potential. We use the notation $I_\sigma = \nabla^2\psi$, where I_σ is evidently the first invariant or the trace of the stress tensor $\boldsymbol{\sigma}$, equal to the stress sum. It is known that the linear invariant of stress (or strain) is a harmonic function in the absence of body forces

$$I_\sigma = \operatorname{tr}(\boldsymbol{\sigma}) = \nabla^2\psi \tag{2.3}$$

From a formal contribution of the 2D Laplace-Operator ∇^2 in equation (2.3), we obtain the Laplace potential equation of the stress sum

$$\nabla^2 I_\sigma = \nabla^2(\sigma_\zeta + \sigma_\xi) = 0 \tag{2.4}$$

where ζ-ξ is any orthonormal basis, By the contribution of the operator ∇^2 in (2.2) with the help of equation (2.3) and rearrangement, we arrive at the Beltrami-Michell equations

$$\sigma_{\alpha\beta,\kappa\kappa} = -I_{\sigma_{\alpha\beta}} + \delta_{\alpha\beta} I_{\sigma_{\kappa\kappa}} \tag{2.5}$$

in which the comma in the subscript indicates partial derivative with respect to the corresponding variables following further on; this notation will be applied in this paper.

This was the second strategy of the theory of elasticity which provides solutions in terms of stress only if the boundary values are known. Note that Beltrami-Michell equations (2.5) are independent of the elastic constants. By examining the three-dimensional kinematic relations, it is found that the exact condition of the state stress in the two-dimensional problems of the elasticity for thin plates exists only if either Poisson's ratio is set equal to zero $(\nu = 0)$ or the surface dilatation is constant and, does not exist except under theses conditions.

This is an important assessment for the photoelasticity especially since it provides that there exists geometric similarity, material isotropy, linearity and similar applied loading of photoelastic specimen and its original. Then the stress distribution per unit load will be identical for each other. In the work by Muskhelishvili (1975) it is emphasized that for the elastic plane on the assumption that the holes contours are free from loading, the stress state does not depend on the elastic characteristics of the material.

From equation (2.5), the following Poisson equations are available to determine the components of the Cartesian stress tensor individually

$$\nabla^2\sigma_x = -I_{\sigma,xx} \qquad \nabla^2\sigma_y = -I_{\sigma,yy} \qquad \nabla^2\tau_{xy} = -I_{\sigma,xy} \tag{2.6}$$

3. Photoelasticity proceeding and associated boundary values

The major task of the numerical treatment of the photoelastic data is the determination of stresses in all interior points of the specimen. However, the photoelastic experiment provides an incomplete solution; only two experimental results $(\sigma_1 - \sigma_2)$ are proportional to the isochromatic order N, and θ for each point, while three stress component parameters are needed to completely define the stress state, sketched in as follows

$$\boldsymbol{\sigma} = \begin{bmatrix} \sigma_x & \tau_{xy} \\ sym. & \sigma_y \end{bmatrix} \Leftrightarrow \begin{cases} N: & \text{isochromatic order} \\ \theta: & \text{slope; isoclinic parameter} \end{cases}$$

The principal stress element (Fig. 1) is used in the prediction of failure surfaces. Potential failure surfaces are the planes on which the maximum normal or maximum shear stress acts; in other words, in the principal planes and the plane of maximum shear.

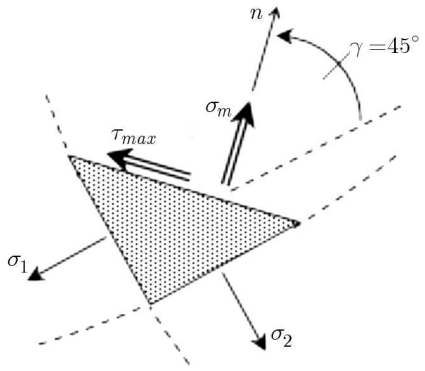

Fig. 1. Principal stress element configuration

The equilibrium of the principal element (Fig. 1) provides the following expressions

$$\sigma_m = \frac{\sigma_1 + \sigma_2}{2} \qquad \tau_{max} = \frac{\sigma_1 - \sigma_2}{2} \tag{3.1}$$

The principal stress σ_1 is by convention the major and σ_2 the minor one ($\sigma_1 > \sigma_2$). The following fundamental equation, (3.2), of photoelasticity, called the stress-optic law (Ramesh, 2000), which stipulates that the relative retardation N, isochromatic fringe order, at each point in the model is directly proportional to the difference of principal stresses $(\sigma_1 - \sigma_2)$ at the point

$$\sigma_1 - \sigma_2 = \frac{N f_\sigma}{t} = \kappa N \tag{3.2}$$

where κ is an experimental constant, quotient of the stress-optical coefficient f_σ, a constant that depends upon the model material and the wavelength of light employed (Ramesh, 2000), and t is the model thickness. We can rewrite the tensor as

$$\boldsymbol{\tau} = \frac{1}{2}\begin{bmatrix} I_\sigma & \kappa N \\ \kappa N & I_\sigma \end{bmatrix} \tag{3.3}$$

This means that the stress tensor $\boldsymbol{\tau}$ relates the centre σ_m and the radius τ_{max} of the Mohr circle. Also in this stress state configuration, the first invariant of the stress tensor of equation (3.3) is verified $I_\sigma = 2\sigma_m$. The stress tensor in relationship (3.3) is often used in order to separate the principal stresses, when its trace is avaible as experimental or numerical data (Kuske, 1979).

To solve the set of partial differential equations (2.4) and (2.6), different kinds of stresses must be available on the boundaries. On the free boundaries, the stress state is generally easy to determine, while difficulties can arise in the loaded ones. The load types are various and each case must be studied individually. When a concentrated load acts on the straight edge of a semi-infinite plate, the stress distribution is purely radial. To have more details on several types of boundary loads, we can refer to Frocht (1948). By definition, the boundaries which are free from external shear and normal stresses will be referred to as free boundaries. The directions of the principal stresses are therefore either tangent or normal to the boundary with the normal stress assumed to be zero. It follows that at the points lying on the free boundaries, there is only one principal stress which is tangent to the boundary.

Since the stress pattern provides the necessary data to calculate $(\sigma_1 - \sigma_2)$ at each point of the free boundary, where either σ_1 or σ_2 vanishes, the stress pattern gives directly the numerical value of the remaining principal stress. The sign of the boundary stress can be easily determined by considering the external loading or by pressure nail control on the boundary (see Wolf, 1976). The required boundary potentials can be easily obtained from photoelastic study of the specimen in which the principal stress sums can be found directly, because they are identical with the principal stress differences on the free boundaries (Doyle, 2004)

$$(\sigma_1 + \sigma_2)\Big|_{\partial\Omega} = (\sigma_1 - \sigma_2)\Big|_{\partial\Omega} \tag{3.4}$$

The equilibrium of forces on an element in plain stress gives a relationship among the Cartesian stress components and the two principal stresses. The boundary equilibrium conditions and the knowledge of photoelasticity of the stress sum $\sigma_x + \sigma_y$ can be coupled to yield the following system

$$\begin{aligned} &\sigma_x n_x + \tau_{xy} n_y = t_x \qquad \tau_{xy} n_x + \sigma_y n_y = t_y \\ &(\sigma_x + \sigma_y)\Big|_{\partial\Omega} = \kappa N(x,y)\Big|_{\partial\Omega} \end{aligned} \tag{3.5}$$

where n_x, n_y are the Cartesian components of the outward normal vector on the surface boundary and t_x, t_y are the Cartesian components of the specified boundary traction. The traction

would be zero for the free boundary, or specified at regions of load application. Knowing the inclination angle θ (or the slope) at a given point on the edge and the tangential stress $\sigma_B = \kappa N(x, y)$ at the same point (see Fig. 2), the components of the Cartesian stresses are computed using separately the equilibrium conditions as follows

$$\sigma_x = \sigma_B \cos^2\theta \qquad \sigma_y = \sigma_B \sin^2\theta \qquad \tau_{xy} = -\sigma_B \sin\theta\cos\theta \tag{3.6}$$

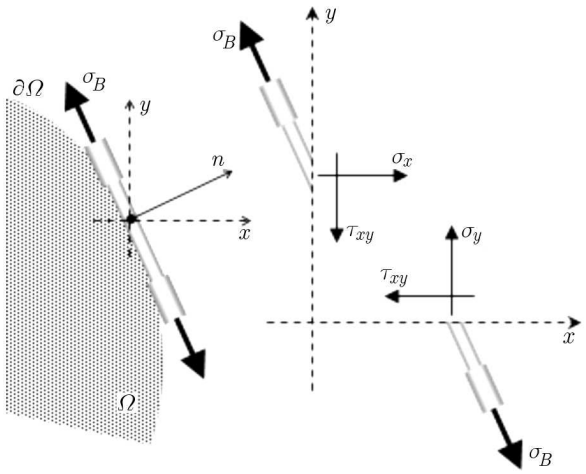

Fig. 2. Tensile state on the free boundary and associated Cartesian stresses

4. Numerical processing on an irregular domain

The motivation of numerical processes to solve partial differential equations is to transform them into algebraic equations by means of finite differences or finite elements, or others. The simplest way is to replace the partial derivatives by discrete finite differences. FDM imposes usually a regular grid on the region of interest where the domain edges coincide with the axis of the coordinate system. This is one of the main disadvantages of FDM where complex geometries cannot be directly resolved by fitting the mesh to the object boundary. The crucial feature of the formulation is FDM discretisation of the homogeneous and mixed derivatives at irregularly shaped boundaries. For this task, many procedures exist; e.g. McKenney *et al.* (1996) proposed a fast Poisson-solver for complex geometries, Zhang (1998) developed a multigrid solution for Poisson's equation.

The Poisson-solvers list is long; a simple method to program is proposed for this task. The finite difference approximation is based on a uniform mesh size, and the resulting system of linear equations is solved by a residual method or multigrid method. A generalized approach is proposed in this paper in order to redefine the finite difference formula taking into account the irregular regions. A varying 5-point stencil is systematically used for the purpose of discretization of the homogeneous and the mixed partial derivatives occurring in both the Laplace equation and in the right-hand-side of the Poisson equation.

To approximate the solution to (2.4) and (2.6), a spatial discretization mostly in irregular geometries, using centred, second order finite-differences as discussed below is used. Let Φ be a generic grid variable used for the approximation. Using the 5-point stencil formula, the following compact algebraic equation at the stencil centres can be written as

$$\sum_{k=0}^{4} \overset{\alpha}{C}_k \Phi_k = \begin{cases} 0 & \text{Laplace} \\ f\big|_{(k=0)} & \text{Poisson} \end{cases} \tag{4.1}$$

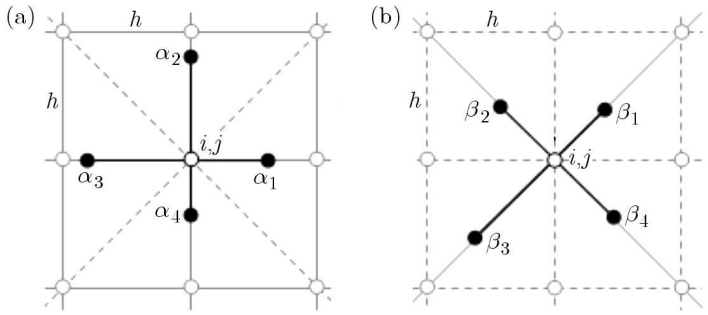

Fig. 3. Irregular 5-point stencils; LHS for homogeneous, RHS for mixed derivatives

In this equation, the coefficients $\overset{\alpha}{C}_k$ regulate the spacing to the boundary $\partial\Omega$, and f represents each right-hand-side of stress component equations (2.6). For grid points far away or close to the boundary, the irregular 5-point discretization operator, introduced early by Shortley and Weller (1938) and still by Sangdong Kim *et al.* (2011), is used. The coefficients of the finite difference equations depend on the spacing to the boundaries. The Shortley-Weller coefficients will be distinctly expressed by

$$\begin{aligned}
&\overset{\alpha}{C}_1 = \frac{1}{h^2\alpha_1(\alpha_1+\alpha_3)} \qquad && \overset{\alpha}{C}_2 = \frac{1}{h^2\alpha_2(\alpha_2+\alpha_4)}\\
&\overset{\alpha}{C}_3 = \frac{1}{h^2\alpha_3(\alpha_3+\alpha_1)} \qquad && \overset{\alpha}{C}_4 = \frac{1}{h^2\alpha_4(\alpha_4+\alpha_2)}\\
&\overset{\alpha}{C}_0 = -\sum_{k=1}^{4}\overset{\alpha}{C}_k
\end{aligned} \tag{4.2}$$

Crucial undertaking is to formulate the discretization of the right-hand-side of the Poisson equation of shear stress, the last of equations (2.6) at the irregular boundaries. The motivation of the following approach is to produce an accurate method for treating mixed derivatives. Near the boundary, the approximation of the second order mixed derivatives requires a 9-point stencil. A transformation by a rotation of $45°$ of the grid (stencil) to obtain a 5-point formula is also recommended. Notice that the 2-dimensional Taylor series approach, according to the approximation of mixed derivatives, leads to the similar form of Shortley-Weller's coefficients by turning over $45°$ the stencil as shown in Fig. 3b. The finite difference coefficients for mixed derivates can be expressed in individual terms as follows

$$\begin{aligned}
&\overset{\beta}{C}_1 = \frac{1}{2h^2\beta_1(\beta_1+\beta_3)} \qquad && \overset{\beta}{C}_2 = \frac{-1}{2h^2\beta_2(\beta_2+\beta_4)}\\
&\overset{\beta}{C}_3 = \frac{1}{2h^2\beta_3(\beta_3+\beta_1)} \qquad && \overset{\beta}{C}_4 = \frac{-1}{2h^2\beta_4(\beta_4+\beta_2)}\\
&\overset{\beta}{C}_0 = -\sum_{k=1}^{4}\overset{\beta}{C}_k
\end{aligned} \tag{4.3}$$

The above symbols α, β are used respectively for the normal and inclined stencil. By definition, the irregular 5-point difference star is present when at least one of its star boughs becomes smaller than the mesh size h. The irregular difference star is the more general case and for the regular star one, $\alpha_k = \beta_k = 1$.

Direct or iterative methods are two different approaches that can be used for solving systems linear equations. In this study, the direct method which produces an exact solution in a finite number of operations is used. The advantages of this method are its numerical robustness and

the fact that it always guarantees a solution for various complex problems without the necessity of a convergence criterion. When solving successively the Laplace and the Poisson systems of equations, the errors in the solutions arise only from rounding off the errors in the computational calculation. This method is tested on several applications examples and is found to produce accurate results.

5. Proceeding in annulus application

Methods for automatic determination of parameters in photoelasticity were validated for the problem of a ring under diametrical load, as for example in Gao (2010), Zhang Dongsheng *et al.* (2002, 2007). Concerning the choice of the results for validation, a particular work is selected as the reference because of its more accurate results. Different methods were developed by Gerlach (1968), later refined by Nurse and Allison (1972); and Redner (1974), who used a standard polariscope with fixed filters. All relevant data for the photoelastic measurement are measured electronically and are the input in a computer via an analogic-digital converter. A program was developed by Gerlach (1968) which enabled complete evaluation of the stresses along the line that had been measured on the model. The most important part of this program is the determination of an isochromatic fringe order from the light intensity distribution (skeletonizing of the fringe). For this, algorithms have been developed to allow exact determination of the fringe order by using two measurements with different wavelengths of light. Other parts of the program have to carry out the curve fit using the method of least squares and to determine the stresses using the Shear-Stress-Difference method. The apparatus built by Gerlach (1968) along with the program made quasi-automatic evaluation of photoelastic data possible. Although this electrical measurement method is the most accurately method used, but it was more expensive.

The photoelastic stress field fringe patterns are shown in Fig. 4. Isochromatic parameters [order] have been superimposed for convenience over the isoclinic parameters in the field along the line that had been measured.

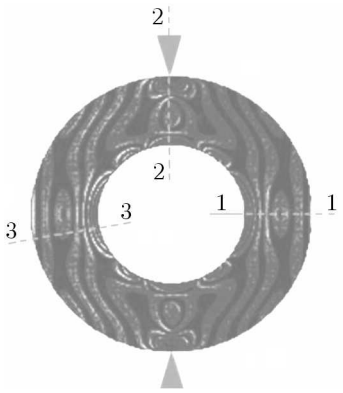

Fig. 4. Photoelastic stress field fringe patterns of the annulus subjected to compressive forces; straight line 3-3 indicates the inclined cross section by 15°)

The stress integration can be started from the initial values, and the stress separation will be accomplished according to numerical integration of one of both equilibrium equations

$$\sigma_x\big|_i = \sigma_x\big|_0 - \sum_0^i \Delta\tau_{xy}\Big(\frac{\Delta x}{\Delta y}\Big) \qquad \sigma_y = \sigma_x \pm \sqrt{(\sigma_1-\sigma_2)^2 - 4\tau_{xy}^2} \tag{5.1}$$

The initial values of stress are obtained from the boundary values at the point from conditions introduced by (3.6). For stress separation along the straight line, the last relation $(5.1)_2$ is

used. In this case, it is important to precise the difference between both procedures: in the SSD-process, the stress component σ_y is determined one from another by means of the Mohr circle statement; while the isoclinic parameter θ is used for the integration. It be noted that determination of the isoclinic parameter θ in its physical range is still a difficult problem. A number of full-field approaches have been proposed to determine it; see details in Ramesh *et al.* (2011), Fernández (2011), Pinit and Umezaki (2005, 2007), and Pinit (2007). The cumulative error in the integration process has also an effect on the stress separation. In the B-M BVP, each stress component occurs from the value on the boundary as BVP separately. In addition, it is noted that the annulus edge direction (slope) is the principal stress direction itself in the case of a free boundary.

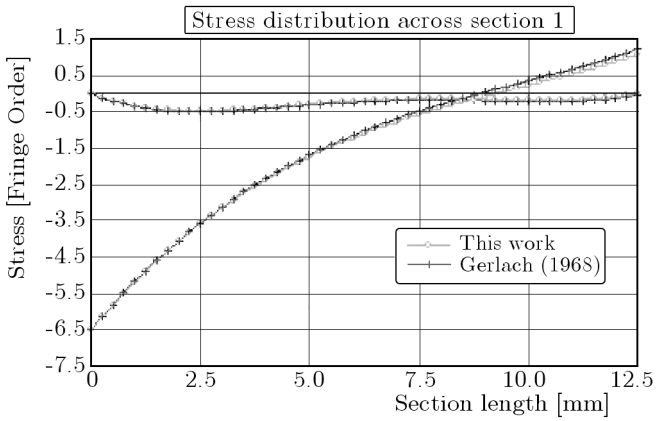

Fig. 5. Radial and tangential stress distributions along section 1 (Gerlach, 1968)

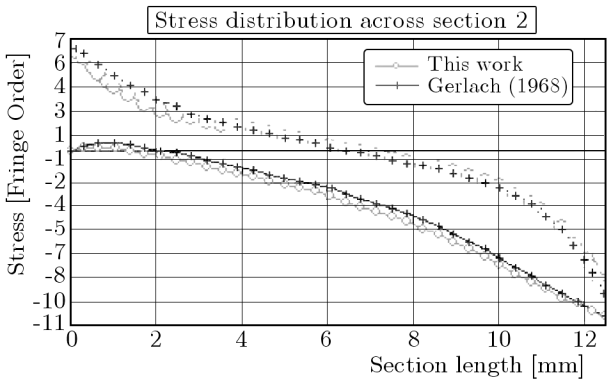

Fig. 6. Radial and tangential stress distributions along section 2 (Gerlach, 1968)

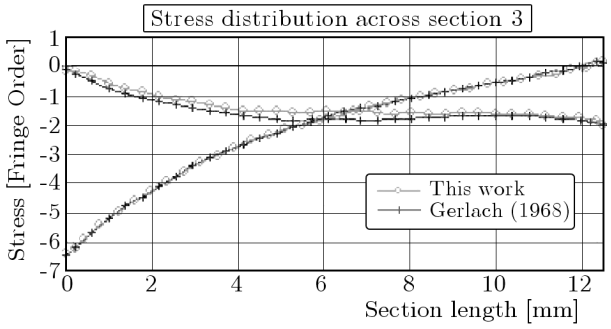

Fig. 7. Radial and tangential stress distributions along section 3 (Gerlach, 1968)

Separating in resulting data in individual components usually provides stresses at only discrete locations. Techniques such as photoelasicity or thermoelasticity also suffer from this consequence of the point-by-point or line-by-line approach. However, discrete data can be converted into appropriate contours. As well as by FEM, post-processor concepts offer a suitable alternate approach to differentiate or help to convert discrete data into maps, particularly for irregularly geometrical shapes. In this purpose, the field results are presented in Figs. 8a,b. On account of symmetry, the different stresses are given as half fields.

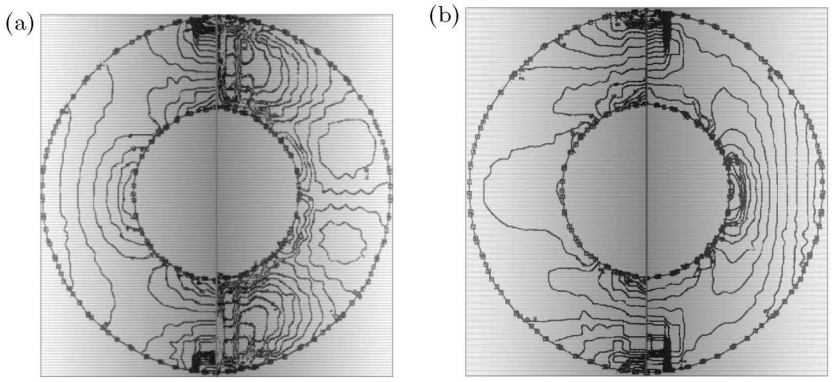

Fig. 8. Non-smoothed; (a) LHS: $(\sigma_1 + \sigma_2)$-maps, RHS: τ_{xy}-maps; (b) LHS: σ_x-maps, RHS: σ_y-maps

Generally, in the experimental analysis, the circular disk under diametral compression is used as the standard model for verification of the performance of any developed method, since the theoretical formula exists for the reconstruction, e.g. of the isochromatic parameters. It has been shown that the results obtained from the hybrid method developed here, provides accurate results for a circular ring.

6. Conclusion

The aim of this paper was to show an efficient additional method for stress separation (see a review by Fernández, 2010). With a minimum cost, the method is faster in proceeding, compared to those suggested in different works by Mahfuz *et al.* (1990), Jacob (1978) and Segerlind (1971). Based on numerical solving of the B-M BVP of Dirichlet type, this method reduces the photoelastic data to minimum, in order to separate the prevailing stresses. It is important to notice that the direct method to solve the system of finite difference equations, despite the sparse matrix, is more qualified to the nature of the experiment in general.

The results of the investigation have shown that the method is easy to use and resolve engineering problems. This method is suitable for automation of the hybrid process of generating stress component maps and enables building the whole stress tensor field. This method is simple enough, so that it can be used with a few equipment elements.

References

1. Boresi A.P., Chong A.P., Lee J.D., 2011, *Elasticity in Engineering Mechanics*, 3rd Ed., John Wiley and Sons, Inc.
2. Doyle J.F., 2004, *Modern experimental stress Analysis*, John Wiley and Sons Ltd.
3. Fernández M.S-B., 2011, Towards uncertainty evaluation in photoelastic measurements, *J. Strain Analysis*, **45**, 275-285

4. Fernández M.S-B., Alegre Calderón J.M., Bravo Diez P.M., Cuesta Segura I.I., 2010, Stress-separation techniques in photoelasticity: a review, *Strain*, **1**, 1-17

5. Filon L.N.G., 1924, The stresses in a circular ring, *Inst. Civil Eng. London: Selected Engineer. Papers*, **1**, 12, 4-26

6. Frocht M.M., 1948, *Photoelasticity*, Vol. II, John Wiley and Sons, New York

7. Gao S., 2010, *In-Plane Stress Analysis using Tensor Field Photoelasticity*, Thesis, University of British Columbia, Vancouver

8. Gerlach H.-D., 1968, *Eleklronische Hilfsmittel zur Automalisierung spannungsoptischer Messungen (Electronic Aids for the Automation of Photoelastic Measurements)*, Doctoral thesis, University of Karlsruhe, FR Germany

9. Hetnarski R.B., Ignaczak J., 2011, *The Mathematical Theory of Elasticity*, Taylor Francis

10. Jacob K.A., 1978, Experimental numerical hybrid technique for stress analysis, *VDI-Berichte*, **335**, 335-341

11. Kuske A., 1979, Separation of principal stresses in photoelasticity by means of a computer, *Strain*, **2**, 43-49

12. Mahfuz H., Caser O., Wong T.-L., 1990, Hybrid stress analysis by digitized photoelastic data and numerical methods, *Experimental Mechanics*, **2**, 90-194

13. McKenney A., Greengard L., Mayo A., 1996, A fast Poisson solver for complex geometries, *Journal of Computation Physics*, **2**, 348-355

14. Muskhelishvili N.I., 1975, *Some Basic Problems of the Mathematical Theory of Elasticity*, 4th Ed. English translation, Noordhoff International Publishing, Leyden

15. Navneet Kumar L., Khobragade N.W., 2011, Analysis of thermal stresses and displacement in a thick annular disc, *Int. J. of Latest Trends in Mathematics*, **2**, 1, 39-46

16. Nomura Y., Pinit P., Umezaki E., 2008, Digital simulation of a circular ring loaded by a diametric compression for photoelastic analysis, *Journal of JSEM*, **8**, Special Issue 83-87

17. Nurse P., Allison I.M., 1972, Automatic acquisition of photoelastic data, *J.B.C.S.A. Conference*

18. Pinit P., 2007, Automated detection of singularities from orientation map of isoclinics in digital photoelasticity, *21st Conf.of Mech. Eng.*, Chonburi, Thailand

19. Pinit P., Umezaki E., 2005, Full-field determination of principal-stress directions using photoelasticity with plane polarized RGB lights, *Optical Review*, **12**, 3, 228-232

20. Pinit P., Umezaki E., 2007, Digitally whole field analysis of isoclinic parameter in photoelasticity by four-step color phase-shifting technique, *Optics and Lasers in Engineering*, **45**, 7, 795-807

21. Ramesh K., 2000, *Digital Photoelasticity: Advanced Techniques and Applications*, Springer

22. Ramesh K., Kasimayan T., Simon B.N., 2011, Digital photoelasticity – A comprehensive review, *Journal of Strain Analysis for Engineering Design*, **46**, 245-266

23. Redner S., 1974, New automatic polariscope system, *Experimental Mechanics*, **14**, 12, 486-491

24. Rezini D., 1984, *Randisochromaten als ausreichende Information zur Spannungstrennung und Spannungsermittlung*, Doctoral thesis, Tech. University of Clausthal (TUC), FR Germany

25. Sangdong Kim, Soyoung Ahn, Philsu Kim, 2011, Local boundary element based a new finite difference representation for Poisson equations, *Applied Mathematics and Computation*, **217**, 12, 5186-5198

26. Sciammarella C.A., Gilbert J.A., 1973, Strain analysis of a disk subjected to diametral compression by means of holographic interferometry, *Applied Optics*, **8**, 12, 1951-1956

27. Segerlind L.J., 1971, Stress-difference elasticity and its application to photomechanics, *Experimental Mechanics*, **11**, 440-445

28. Shortley G.H., Weller R., 1938, The numerical solution of Laplace's equation, *Appl. Phys.*
29. Timoshenko S.P., Goodier J.N., 1970, *Theory of Elasticity*, 3-rd Ed., New York, Mc-Graw Hill
30. Tokovyy Yu.V., Hung K.-M., Ma C.-C., 2010, Determination of stresses and displacements in a thin annular disk subjected to diametral compression, *J. of Math. Sciences*, **3**, 342-354
31. Ugural A.C., Fenster S.K., 2011, *Advanced Mechanics of Materials and Applied Elasticity*, 5-th Ed., Prentice Hall
32. Wolf H., 1976, *Spannungsoptik, Band 1 Grundlagen. Zweite Auflage*, Springer
33. Zhang Dongsheng, Min Maa, Dwayne D. Arola., 2002, Fringe skeletonizing using an improved derivative sign binary method, *Optics and Lasers in Eng.*, **37**, 51-62
34. Zhang Dongsheng, Yongsheng Han, Bao Zhang, Dwayne Arola, 2007, Automatic determination of parameters in photoelasticity, *Optics and Lasers in Eng.*, **45**, 860-867
35. Zhang J., 1998, Fast and high accuracy multigrid solution of the three dimensional Poisson equation, *Journal of Computation Physics*, **2**, 449-461

Wyznaczanie pierwszej wartości brzegowej w zagadnieniu fotoelastyczności cienkiego pierścienia

Streszczenie

Analityczne rozważania płaskiego stanu naprężeń w cienkich strukturach pierścieniowych poddanych obciążeniu ściskającemu są szeroko znane w literaturze. Co więcej, większość przypadków tego typu zagadnień teorii sprężystości daje się zredukować do problemu wyznaczania wartości własnych zagadnienia brzegowego. Metody dwuwymiarowej fotoelastyczności umożliwiają łatwą identyfikację składowych tensora naprężeń na brzegu elementu w oparciu o pojedynczą fotografię. Równania Beltramiego-Michella warz z parametrami fotoelastyczności Dirichleta pozwalają poprawnie sformułować hybrydowy model badanego układu w kontekście poszukiwanych naprężeń. W pracy wykazano, że taki model jest stosowalny do dowolnie nieregularnego kształtu próbki. Otrzymano bardzo dobre wyniki dla elementów o skomplikowanym obrysie i poddanych złożonemu stanowi obciążenia. W szczegółowej analizie potwierdzono dokładność rezultatów dla pierścienia kołowego.

Manuscript received February 29, 2012; accepted for print April 11, 2012